ISSN 0023-1584, Kinetics and Catalysis, 2009, Vol. 50, No. 2, pp. 156–161. © Pleiades Publishing, Ltd., 2009.
Original Russian Text © O.P. Korobeinichev, A.G. Shmakov, I.V. Rybitskaya, T.A. Bol'shova, A.A. Chernov, D.A. Knyaz'kov, A.A. Konnov, 2009, published in Kinetika i Kataliz, 2009, Vol. 50, No. 2, pp. 170–175.

Kinetics and Mechanism of Chemical Reactions in the $H_2/O_2/N_2$ Flame at Atmospheric Pressure

O. P. Korobeinichev, A. G. Shmakov, I. V. Rybitskaya, T. A. Bol'shova, A. A. Chernov, D. A. Knyaz'kov, and A. A. Konnov

e-mail: korobein@kinetics.nsc.ru

Received March 26, 2008; in final form, April 24, 2008

Abstract—The kinetics and mechanism of chemical reactions in the $H_2/O_2/N_2$ flame were studied experimentally and by simulating the structure of premixed laminar flat atmospheric $H_2/O_2/N_2$ flames of different initial compositions. The concentration profiles for stable compounds (H_2, O_2, and H_2O), H atoms, and $OH^{\bullet}$ radicals in flames were measured by molecular-beam sampling mass spectrometry using soft electron-impact ionization. The experimental data thus obtained are in good agreement with the results of simulations in terms of three familiar kinetic mechanisms, suggesting that these mechanisms are applicable to the description of the flame structure in hydrogen–oxygen mixtures at atmospheric pressure.

DOI: 10.1134/S0023158409020025

The mechanism and chemistry of the combustion and ignition of hydrogen/oxygen mixtures have been the subject of detailed studies for many years. One of the causes of this interest is that the combustion and ignition of these mixtures provide glowing examples of branched chain reactions, which were discovered by N.N. Semenov and were investigated in detail by his followers [1–6]. Numerous modifications of the kinetic mechanism of hydrogen ignition and combustion have been suggested to date [1–16], and they have proved convincingly that the reactions proceed via a chain mechanism. However, the authors of a recent publication [17] deny the branched chain character of hydrogen ignition and combustion at near-atmospheric pressures. The advances in the understanding of the mechanisms of chemical reactions in flames have been made by comparing experimental data (propagation rate, ignition delay, flame structure, etc.) collected over the widest possible ranges of conditions (pressure temperature, the initial composition of the reaction mixture) with the results of numerical calculations for the trial mechanisms.

The determining role in branched chain processes is played by reactions involving active species, namely, atoms and free radicals. Therefore, the most important and most complicated problem is to measure their concentrations and to record their concentration profiles in the flame. Molecular-beam sampling mass spectrometry (MBSMS) with soft electron-impact ionization is among the most efficient methods used for this purpose. Eltenton [14] and, later, Foner and Hudson [15] were the first to apply this method to the detection of atoms and radicals in rarefied flames. MBSMS, which is the most universal method from the standpoint of simultaneous measurement of the concentrations of all compounds in the flame, including atoms and free radicals, is widely used in the study of the flame structure, including for hydrogen–oxygen mixtures. Most of the studies of the structure of these flames deal with subatmospheric pressures [16, 18–20] because of the difficulties in the use of the MBSMS method at $P = 1$ atm. Nevertheless, there have been several studies on the structure of hydrogen/oxygen flames at atmospheric pressure and above [21–23]. These studies provided concentration profiles only for stable compounds in rich [21, 22] and stoichiometric [23] flames. For detailed and comprehensive verification of the kinetic mechanism of the chemical reactions involved in hydrogen combustion at 1 atm, it is necessary to have concentration distribution data for the active species H and $OH^{\bullet}$ in these flames. Here, we report a development in testing a soft electron-impact ionization MBSMS technique for flame structure studies (primarily for measuring the H and $OH^{\bullet}$ concentrations and concentration profiles) at atmospheric pressure and the application of this technique to "atmospheric" $H_2/O_2/N_2$ flames having different stoichiometries. A comparison between the results of this experiment and the results of simulation for mechanisms known from the literature would make it clear whether these mechanisms are valid.

EXPERIMENTAL

In order to perform experiments under conditions close to the adiabatic conditions of free flame propagation, we used a technique ensuring heat flux balance (HFB) on the burner [24, 25]. The burner was a tube 35 cm in height on which a copper disc 24 mm in diameter and 3 mm in thickness was mounted. The disc had

uniformly arranged 0.5-mm holes separated by a distance of 0.7 mm from one another. The copper disc and the combustible mixture were heated along the outer perimeter of the burner using circulating water from thermostats. The disc edge temperature was maintained at 60°C; the mixture (hydrogen/oxygen/nitrogen) temperature, at 35°C. The flow velocity of the initial combustible mixture for $\phi = 1.1$ and 2.0 ($\phi = [H_2]/[H_2]_{stoich}$) was set 1–4 cm/s below the flame propagation velocity determined by the HFB method using the same burner. The $\phi = 0.47$ flame has a cellular structure. In order to avoid this phenomenon, its structure was determined at a flow velocity lower by 40% than the free flame propagation velocity. The composition and flow rate of combustible mixtures were set using mass flow controllers (MKS Instruments Inc.). The purity of the gases (H_2, O_2, and N_2) was 99.95%.

In order to measure the radial temperature distribution on the burner surface, we soldered copper–constantan thermocouples into the burner holes at distances of 0, 2.4, 4.5, 7.0, 10.0, and 12.0 mm from the burner axis. For flame stabilization under near-adiabatic conditions and for measuring the flame propagation velocity, we used the HFB method [24, 25]. In this method, the velocity of the gas flowing through the burner is adjusted so that heat transfer to the burner is compensated for by the controlled heating of the mixture, so the heat loss balance (determined using microthermocouples built into the burner surface) is close to zero.

For flame stabilization in the study of the flame structure, the mixture flow velocity was set somewhat below the free flame propagation velocity. For the calibration flame, the mixture flow velocity was 42.5 cm/s and the free propagation velocity was 47 cm/s. The initial conditions, mixture compositions, and flame propagation velocities calculated using special-purpose programs [26–28] for the mechanism presented in [8] are listed in the table.

Experimental conditions

Parameter	Rich flame	Calibration flame	Lean flame
$\phi = [H_2]/[H_2]_{stoich}$	2	1.1	0.47
$D = [O_2]/([O_2] + [N_2])$	0.077	0.090	0.209
$[H_2]$, mole fraction	0.2355	0.1653	0.1642
$[O_2]$, mole fraction	0.0589	0.0751	0.1747
$[N_2]$, mole fraction	0.7056	0.7596	0.6611
Experimental flame velocity at the burner surface, cm/s	40.70	42.50	34.24
Experimental free flame propagation velocity, cm/s	41.1	47.0	55.0
Free flame propagation velocity calculated using the mechanism reported in [8], cm/s	39.6	38.3	36.2

The temperature profile in the flame was measured with a SiO_2-coated Pt/(Pt + 10% Rh) thermocouple 0.02 mm in diameter. The junction of the thermocouple was placed at a distance of 0.2 mm from the tip of the probe to take into account the perturbations caused by the probe. The temperature profile thus measured was used in simulations via the programs presented in [26–28].

The sampler is known to perturb the flame structure. This perturbation consists of thermal and gas-dynamic effects. The thermal perturbation is flame cooling by the sampler. In order to take into account this perturbation, we measured temperature profiles with a thin thermocouple (~0.04 mm in diameter) placed at a fixed distance (0.2 mm) from the sampler hole and introduced these profiles into the calculation of concentration profiles in the flame via the above-mentioned programs [26–28]. The gas-dynamic perturbation of the flame by the probe was taken into account by "shifting" the measured concentration profiles in the flow upward relative to the measured temperature profile and relative to the calculated concentration profiles. The value of this shift, ΔZ, was estimated using the following semiempirical formula [29]: $\Delta Z = 0.37d\sqrt{\frac{Q}{SV}}$, where d is the diameter of the probe hole, Q is the gas flow rate in the probe hole, S is the cross sectional area of the probe hole, and V is the velocity of the incoming gas flow. The maximum shift corresponds to the shortest distance between the probe and the burner surface and is 0.3 mm.

The concentration profiles of substances were measured using a molecular-beam sampling system and an MS7302 quadrupole mass spectrometer equipped with an improved ion source ensuring soft ionization [30]. The burning gas was sampled at various distances from the burner surface using a quartz probe with a hole diameter of 0.08 mm and a divergence angle of 40°. The concentration profiles were obtained using calibration coefficients for the observed species. For the stable components of the flame (O_2 and H_2O), these coefficients were determined by direct calibration. To do this, we measured the intensities of the corresponding principal ion peaks (m/z = 32 and 18) for air containing water vapor heated to 200°C. Argon, which is a component of air, provided a reference peak. Calibration coefficients (k_i) versus that of argon were calculated using the formula

$$k_i = C_i I_{40}/C_{Ar} I_i, \quad (1)$$

where I_i and I_{40} are the intensities of the mother ion peak of the ith compound and argon, respectively, and C_i and C_{Ar} are the mole fractions of the compound being calibrated and argon, respectively.

The concentrations of atoms and radicals in the flame were measured at an electron-impact ionization energy of 16.2 eV. The H, O, and $OH^{\bullet}$ concentrations in

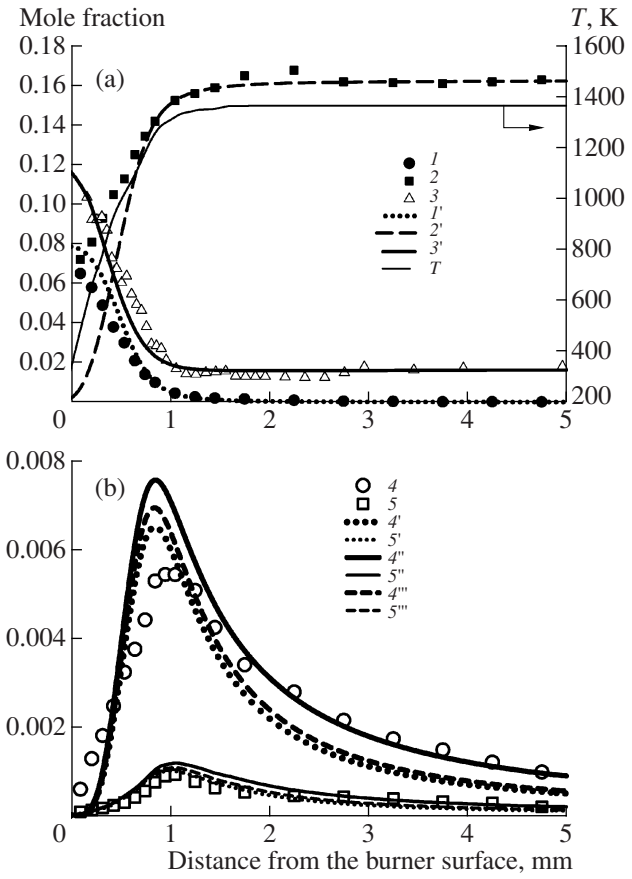

Fig. 1. (a) Temperature profiles and concentration profiles for stable compounds in the $H_2/O_2/N_2$ flame with $\phi = 1.1$ and $D = 0.09$: (*1*, *1'*) O_2, (*2*, *2'*) H_2O, and (*3*, *3'*) H_2. (b) Concentration profiles of (*4*, *4'*, *4''*, *4'''*) H atoms and (*5*, *5'*, *5''*, *5'''*) $OH^\bullet$ radicals in the same flame. The symbols stand for experimental data, and the lines represent the results of the simulations using the mechanisms presented in (*4'*, *5'*) [8], (*4''*, *5''*) [34], and (*4'''*, *5'''*) [7].

the flame were derived from the intensities of the corresponding peaks in the mass spectrum by the well-known method [31] that we used earlier for subatmospheric hydrogen/oxygen flames [32]. This method is based on the fact that detailed balancing among the following three fast reactions takes place in the combustion product zone in hydrogen flames:

$$H_2 + OH^\bullet = H_2O + H, \quad \text{(I)}$$

$$H_2 + O = H + OH^\bullet, \quad \text{(II)}$$

$$O_2 + H = OH^\bullet + O. \quad \text{(III)}$$

The corresponding equilibrium constants K_1, K_2, and K_3 are as follows [33]:

$$K_1 = 0.113T^{0.0839}e^{7680/T}, \quad (2)$$

$$K_2 = 1.8T^{0.027}e^{-917/T}, \quad (3)$$

$$K_3 = 302T^{-0.374}e^{-8620/T}. \quad (4)$$

In this approximation, the expressions for the H, O, and $OH^\bullet$ concentrations appear as

$$[OH^\bullet] = \sqrt{K_2K_3[O_2][H_2]}, \quad (5)$$

$$[O] = \frac{K_1K_3[H_2][O_2]}{[H_2O]}, \quad (6)$$

$$[H] = \frac{K_1[H_2]}{[H_2O]}\sqrt{K_2K_3[O_2][H_2]}. \quad (7)$$

In order to determine the concentrations of radicals and derive calibration coefficients for the radicals H, O, and $OH^\bullet$ from the concentration data, we measured the H_2, O_2, and H_2O concentrations and flame temperatures at several distances from the burner surface.

The H_2 concentration in the zone of final combustion products was determined chromatographically. The hydrogen concentration in this zone is almost invariable. The microprobe hole diameter was 0.08 mm, the outer microprobe diameter at the hole was 0.12 mm, and the tip angle was 20°. The flame gas was sampled into a prepumped glass vessel until a pressure of 301 Torr was reached. Thereafter, the sample was diluted with nitrogen to a pressure of 756 Torr. During sampling, water vapor was frozen out into a liquid-nitrogen trap placed between the microprobe and the glass vessel.

Using formulas (5)–(7), the concentrations of stable compounds, and the equilibrium constants, we calculated the H, O, and $OH^\bullet$ concentrations in the flame for $\phi = 1.1$ and $D = 0.09$ ($D = [O_2]/([O_2] + [N_2])$) in the final combustion product zone. Based on these data, we determined the calibration coefficients for H and $OH^\bullet$. We were unable to determine the calibration coefficient for oxygen atoms with a sufficient degree of accuracy because of their low concentration in the final combustion product zone. According to our estimates, the relative accuracy of the atom and radical concentrations derived in this study from mass spectrometric peak intensities varies between 40 and 60% over the combustion zone.

SIMULATION

The flame propagation velocity was simulated using the program packages PREMIX and CHEMKIN-II [26–28], which allow multicomponent laminar flames to be described taking into account their thermodynamics, kinetics, and transport properties and detailed reaction mechanisms.

Three reaction mechanisms [7, 8, 34] were used in the calculations. The multicomponent diffusion and thermal diffusion of compounds in the flame were taken into account; GRAD = 0.02 and CURV = 0.5.

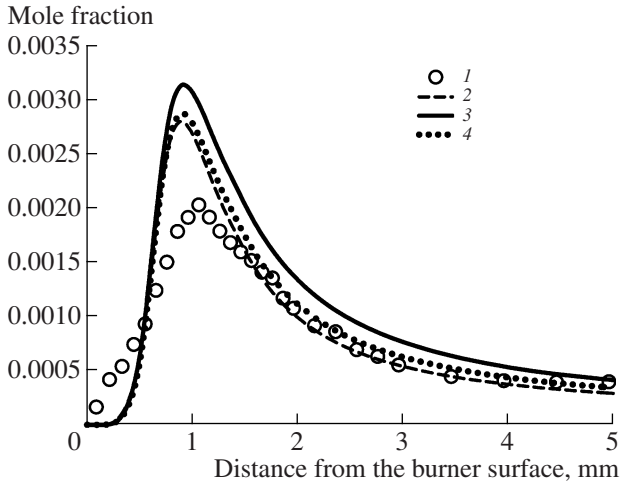

Fig. 2. $OH^\bullet$ concentration profiles in the $H_2/O_2/N_2$ flame ($\phi = 0.47$, $D = 0.209$): (*1*) experiment and (*2–4*) results of numerical simulations using the mechanisms presented in [7], [34], and [8], respectively.

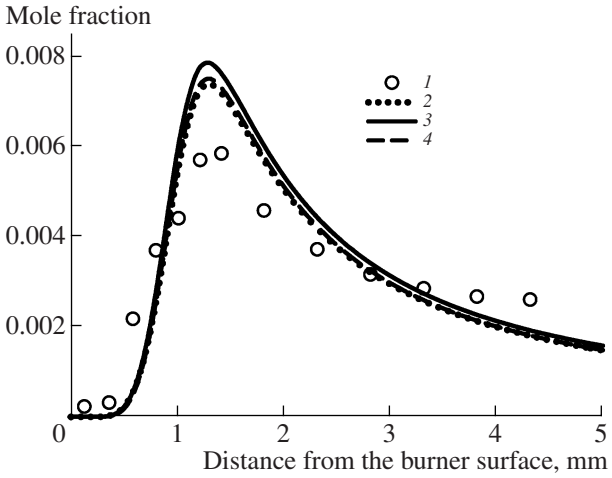

Fig. 3. H atom concentration profiles in the $H_2/O_2/N_2$ flame ($\phi = 2.0$, $D = 0.077$): (*1*) experiment and (*2–4*) results of numerical simulations using the mechanisms presented in [7], [34], and [8], respectively.

RESULTS AND DISCUSSION

Figures 1–3 show concentration profiles for the stable compounds (H_2O, H_2, and O_2), H, and $OH^\bullet$ measured in $\phi = 1.1$, 0.47, and 2.0 flames, respectively. The same figures present the results of the numerical simulation of the flame structure using the three different hydrogen oxidation mechanisms [7, 8, 34]. For all three mechanisms, the calculated concentration profiles of the stable compounds are in good agreement with experimental data. The small discrepancy between the experimental and calculated H_2O concentration profiles near the burner surface is due to the fact that the calibration coefficient for H_2O varies with flame temperature because of the formation of H_2O clusters in the molecular beam in gas sampling from the low-temperature zone of the flame. Thus, the overestimation of the H_2O concentration near the burner surface in our experiments arises from experimental errors.

The $OH^\bullet$ concentration profiles measured in the $\phi = 0.47$ and 1.1 flames are in satisfactory agreement with the results of numerical simulation (Figs. 1b, 2). Note that the measured $OH^\bullet$ concentration peak is shifted toward the final combustion product zone by ~0.10–0.13 mm relative to the calculated peak. The maximum $OH^\bullet$ mole fractions measured in the $\phi = 0.47$ and 1.1 flames are 2.0×10^{-3} and 9.1×10^{-4}, respectively, 20–30% below the corresponding calculated values.

The H concentration profiles measured in the $\phi = 1.1$ and 2.0 flames (Figs. 1b, 3) are also in satisfactory agreement with the calculated data. As in the case of $OH^\bullet$, the observed H concentration peak is slightly shifted (by 0.10–0.13 mm) relative to the calculated peak. This shift is due to the errors in taking into account the perturbations caused by the sampler. The maximum H mole fractions measured in the $\phi = 1.1$ and 2.0 flames are 5.4×10^{-3} and 5.9×10^{-3}, respectively, 16–30% below the corresponding calculated values. The equilibrium H mole fractions calculated for 1250 and 1160 K, the temperatures at which the H concentration peaks in the $\phi = 1.1$ and 2.0 flames take place, are 6.14×10^{-8} and 3.2×10^{-8}, respectively.

Thus, our experimental data are in satisfactory agreement with the results of the calculations, the discrepancy being within the experimental error. The observed high, above-equilibrium concentrations of intermediates are direct evidence of the branched chain character of the reactions in the atmospheric hydrogen flame and prove the correctness of the kinetic mechanisms used in this study, as well as the correctness of the methods developed for active species concentration measurement in flames. An analysis of the sensitivity of the calculated free propagation velocity of the atmospheric $H_2/O_2/N_2$ flame with $\phi = 1.1$ and $D = 0.09$ (whose structure was studied in our experiments; Fig. 1) to the rate constants of the elementary steps included in the kinetic mechanisms demonstrated that the most significant recombination reactions are $HO_2^\bullet + OH^\bullet = H_2O + O_2$, $H + H + M = H_2 + M$, $HO_2^\bullet + H = H_2 + O_2$, $H + O_2(+M) = HO_2^\bullet(+M)$, and $H + OH^\bullet + M = H_2O + M$. These reactions reduce the flame propagation velocity (Fig. 4). The most significant reactions increasing the flame propagation velocity are $HO_2^\bullet + H = OH^\bullet + OH^\bullet$, $OH^\bullet + H_2 = H + H_2O$, $O + H_2 = H + OH^\bullet$, and $H + O_2 = O + OH^\bullet$. Similar results for $H_2/O_2/N_2$ flames of other compositions were obtained by numerical simulation in other studies [35–37].

The rate profiles for the most significant elementary steps and the temperature profiles for the freely propagating flame ($\phi = 1.1$, $D = 0.09$), presented in Fig. 5, are consistent with the analysis of the sensitivity of the

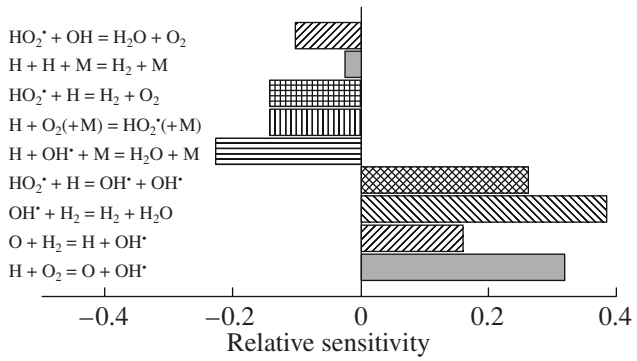

Fig. 4. Relative sensitivity of the propagation velocity of the $H_2/O_2/N_2$ flame ($\phi = 1.1$, $D = 0.09$) to the rate constants of the most significant elementary steps.

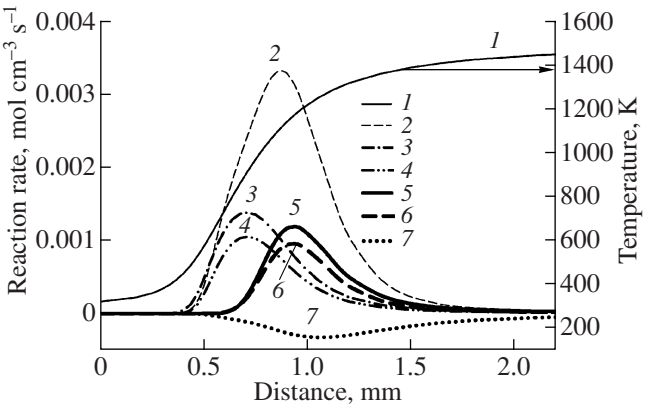

Fig. 5. Temperature profile and rate profiles for the most significant elementary steps for the flame with $\phi = 1.1$ and $D = 0.09$: (*1*) temperature, (*2*) $OH^\bullet + H_2 = H + H_2O$, (*3*) $H + O_2 (+M) = HO_2^\bullet (+M)$, (*4*) $HO_2^\bullet + H = OH^\bullet + OH^\bullet$, (*5*) $H + O_2 = O + OH^\bullet$, (*6*) $O + H_2 = H + OH^\bullet$, and (*7*) $H_2O + M = H + OH^\bullet + M$.

flame propagation velocity to the rate constants of the elementary steps.

Thus, using molecular-beam mass spectrometry with soft electron-impact ionization, we measured, for the first time, the H and $OH^\bullet$ concentration profiles in flames with different hydrogen excess factors at 1 atm. The high concentrations of intermediates measured in this study are direct evidence of the branched chain character of the reactions in the atmospheric hydrogen flame. The experimental data are in good agreement with the results of the numerical simulation of the flame structure in terms of three different hydrogen combustion mechanisms. It was demonstrated that molecular-beam mass spectrometry is applicable to the detection of atoms and free radicals in the investigation of ignition and combustion at atmospheric pressure.

REFERENCES

1. Semenov, N.N., *O nekotorykh problemakh khimicheskoi kinetiki i reaktsionnoi sposobnosti* (On Some Problems of Chemical Kinetics and Reactivity), Moscow: Akad. Nauk SSSR, 1958.
2. Nalbandyan, A.V. and Voevodskii, V.V., *Mekhanizm okisleniya i goreniya vodoroda* (Mechanism of Hydrogen Oxidation and Combustion), Moscow: Akad. Nauk SSSR, 1949.
3. Azatyan, V.V., Doctoral (Chem.) Dissertation, Moscow: Inst. Chem. Phys., 1978.
4. Petrova, L.D., Baratov, A.N., Azatyan, V.V., Kaganova, Z.I., and Makeev, V.I., *Gorenie i vzryv* (Combustion and Explosion), Moscow: Nauka, 1976.
5. Ivanova, A.N., Andrianova, Z.S., and Azatyan, V.V., *Khim. Fiz.*, 1998, vol. 17, no. 8, p. 91.
6. Azatyan, V.V., Andrianova, Z.S., and Ivanova, A.N., *Zh. Fiz. Khim.*, 2006, vol. 80, no. 7, p. 1194 [*Russ. J. Phys. Chem. A* (Engl. Transl.), vol. 80, no. 7, p. 1044].
7. Li, J., Zhao, Z., Kazakov, A., and Dryer, F.L., *Int. J. Chem. Kinet.*, 2004, vol. 36, p. 566.
8. Conaire, M.O., Curran, H.J., Simmie, J.M., Pitz, W.J., and Westbrook, C.K., *Int. J. Chem. Kinet.*, 2004, vol. 36, p. 603.
9. Konnov, A.A., *Khim. Fiz.*, 2004, vol. 23, no. 8, p. 5.
10. Zsely, I.Gy., Zador, J., and Turanyi, T., *Proc. Combust. Inst.*, 2005, vol. 30, p. 1273.
11. Davis, A.G., Joshi, A.V., Wang, H., and Egolfopoulos, F., *Proc. Combust. Inst.*, 2005, vol. 30, p. 1283.
12. Del Alamo, G., Williams, F.A., and Sanchez, A.L., *Combust. Sci. Technol.*, 2004, vol. 176, p. 1599.
13. Saxena, P. and Williams, F.A., *Combust. Flame*, 2006, vol. 145, p. 316.
14. Eltenton, G.C., *J. Chem. Phys.*, 1942, vol. 10, p. 403.
15. Foner, S. and Hudson, R., *J. Chem. Phys.*, 1953, vol. 21, p. 1374.
16. Bascombe, K.N., *Proc. Combust. Inst.*, 1965, vol. 10, p. 55.
17. Aleksandrov, E.N., Kuznetsov, N.M., and Kozlov, S.N., *Fiz. Goreniya Vzryva*, 2007, vol. 43, no. 5, p. 44.
18. Brown, N.J., Eberius, K.H., Fristrom, R.M., Hoyermann, K.H., and Wagner, H.Gg., *Combust. Flame*, 1978, vol. 33, p. 151.
19. Vandooren, J. and Bian, J., *Proc. Combust. Inst.*, 1990, vol. 23, p. 839.
20. Korobeinichev, O.P., Shvartsberg, V.M., Il'in, S.B., Chernov, A.A., and Bol'shova, T.A., *Fiz. Goreniya Vzryva*, 1999, vol. 35, no. 3, p. 29.
21. Dixon-Lewis, G., Sutton, M.M., and Williams, A., *Proc. Combust. Inst.*, 1965, vol. 10, p. 495.
22. Dixon-Lewis, G., Sutton, M.M., and Williams, A., *Proc. R. Soc. London, Ser. A*, 1970, vol. 317, p. 227.
23. Paletskii, A.A., Kuibida, L.V., Bol'shova, T.A., Korobeinichev, O.P., and Fristrom, R.M., *Fiz. Goreniya Vzryva*, 1996, vol. 32, no. 3, p. 3.
24. De Goey, L.P.H., van Maaren, A., and Quax, R.M., *Combust. Sci. Technol.*, 1993, vol. 92, p. 201.
25. Van Maaren, A., Thung, D.S., and de Goey, L.P.H., *Combust. Sci. Technol.*, 1994, vol. 96, p. 327.

26. Kee, R.J., Rupley, F.M., and Miller, J.A., *Sandia National Laboratories Report SAND89–8009*, Livermore: Sandia National Laboratories, 1989.

27. Kee, R.J., Grcar, J.F., Smooke, M.D., and Miller, J.A., *Sandia National Laboratories Report SAND85–8240*, Livermore: Sandia National Laboratories, 1992.

28. Lutz, A.E., Kee, R.J., and Miller, J.A., *Sandia National Laboratories Report SAND87–8248*, Livermore: Sandia National Laboratories, 1990.

29. Korobeinichev, O.P., Tereshchenko, A.G., and Emel'yanov, I.D., *Prepr. of Inst. of Chemical Kinetics and Combustion, Inst. of Theoretical and Applied Mechanics, and Novosibirsk State Univ.*, Novosibirsk, 1985, no. 14.

30. Korobeinichev, O.P., Ilyin, S.B., Shvartsberg, V.M., and Chernov, A.A., *Combust. Flame*, 1999, vol. 118, no. 4, p. 718.

31. Warnatz, J., *Combust. Sci. Technol.*, 1981, vol. 26, p. 203.

32. Korobeinichev, O.P., Shvartsberg, V.M., and Chernov, A.A., *Combust. Flame*, 1999, vol. 118, no. 4, p. 727.

33. Baulch, D.L., Bowman, C.T., Cobos, C.J., Cox, R.A., Just, Th., Kerr, J.A., Pilling, M.J., Stocker, D., Troe, J., Tsang, W., Walker, R.W., and Warnatz, J., *J. Phys. Chem. Ref. Data*, 2005, vol. 34, no. 3, p. 757.

34. Konnov, A.A., *Detailed Reaction Mechanism for Small Hydrocarbons Combustion*, Release 0.5, http://homepages.vub.ac.be/~akonnov/, 2000.

35. Marinov, N.M., Westbrook, C.K., and Pitz, W.J., *8th Int. Symp. on Transport Properties*, San Francisco, 1995.

36. Dong, Y., Holley, A.T., Andac, M.G., Egolfopoulos, F.N., Davis, S.G., Middha, P., and Wang, H., *Combust. Flame*, 2005, vol. 142, no. 4, p. 374.

37. Egolfopoulos, F.N. and Law, C.K., *Proc. Combust. Inst.*, 1990, vol. 23, p. 333.